

ACOUSTIC MODELLING OF A CONVEX PIPE ADAPTED FOR DIGITAL WAVEGUIDE SIMULATION

Rémi Mignot*

Institut Langevin, ESPCI ParisTech
10, rue Vauquelin,
75005 Paris, France
remi.mignot@espci.fr

Thomas Hélie

IRCAM & CNRS, UMR 9912
1, pl. Igor Stravinsky,
75004 Paris, France
thomas.helie@ircam.fr

Denis Matignon

ISAE, Applied Mathematics Training Unit,
10, av. E. Belin, B.P. 54032.
F-31055 Toulouse cedex4, France
denis.matignon@isae.fr

ABSTRACT

This work deals with the physical modelling of acoustic pipes for real-time simulation, using the “Digital Waveguide Network” approach and the horn equation. With this approach, a piece of pipe is represented by a two-port system with a loop which involves two delays for wave propagation, and some subsystems without internal delay. A well-known form of this system is the “Kelly-Lochbaum” framework, which allows the reduction of the computation complexity. We focus this work on the simulation of pipes with a convex profile. But, using the “Kelly-Lochbaum” framework with the horn equation, two problems occur: first, even if the outputs are bound, some substates have their values which diverge; second, there is an infinite number of such substates. The system is then unstable and cannot be simulated as such. The solution of this problem is obtained with two steps. First, we show that there is a simple standard form compatible with the “Waveguide” approach, for which there is an infinite number of solutions which preserve the input/output relations. Second, we look for one solution which guarantees the stability of the system and which makes easier the approximation in order to get a low-cost simulation.

1. INTRODUCTION

Contrarily to some accepted ideas, the case of convex pipes is frequent for wind instruments. We can meet this case at the end of some resonators: e.g. the oboe d’amore (cf. Fig. 1), the English horn, the bassoon, the recorder, and some primitive or non-western instruments. Besides, the vocal tract has some convex parts. Hence, for the application of musical sound synthesis or artificial speech production it is useful to study this particular case.

In [1] and [2], the physical modelling of acoustic wave propagation in convex pipes has been studied, and these studies have shown the presence of trapped modes. Similarly to the model of cone connections with a negative change of slope (cf. e.g. [3]), some problems of stability occur. Nevertheless these instabilities

have no influence in a *global* point of view, and for the simulation some solutions have consisted in considering the system in a global point of view, using for example a modal approach or a digital convolution with finite impulse response filters.

But, for digital simulations with low-cost computations, the modal approaches need the truncation of modes, which involve some problems of realism. And because of some long memory effects (of the diffusive type for visco-thermal losses for example) the convolution methods are not adapted because the impulse responses decrease very slowly.

In [4], flared pipes have been modelled with the *Digital Waveguide Network* approach (cf. e.g. [5]) using the horn equation of Webster (cf. [6]) and taking into account the visco-thermal losses (cf. [7, 8]). The simulation framework of *Kelly-Lochbaum* has been obtained (cf. e.g. [9]). This system involves some delays for wave propagation through pieces of pipe, and some recursive filters for reflections and transmissions at junctions of pieces of pipe. This model leads to real-time simulations. Nevertheless, the application of the latter model to convex pipes produces some stability problems. The aim of this work is to get a stable digital realization for convex pipes, similar to the one of [4].

This paper is organized as follows. Section 2 presents the acoustic model we use, the *Webster-Lokshin* model, and two equivalent systems for the simulation. In sec. 3, we study in the Laplace domain the singularities of the transfer functions involved in this model. In the case of convex pipes, some of these singularities produce unstable substates, then the reason of their presence is explained. To solve this problem, first, in sec. 4 we propose a “generalized” framework. It describes the acoustic pipe with 2 degrees of freedom which are 2 transfer functions of the system. Hence, we can parameterize the modelling and we get an infinite number of solutions which preserve the input/output relations. Second,



Figure 1: Oboe d’amore (cf. [10]).

* This work has been realized at the IRCAM during the Ph.D. thesis of Rémi Mignot. It has been supported by the CONSONNES project, ANR-05-BLAN-0097-01.

in sec. 5 we search for 2 transfer functions (degrees of freedom) which allow a stable digital simulation for convex pipes. The proposed choice is compatible with the *Waveguide* approach and it is similar to [4]. The last section concludes this paper and deals with perspectives.

2. ACOUSTIC MODEL AND SYSTEMS

2.1. The Webster-Lokshin model

The *Webster-Lokshin* model is a mono-dimensional model which characterizes the linear propagation of acoustic waves inside axisymmetric pipes, with the weak hypothesis of quasi-sphericity of isobars near the wall (cf. [8]), and taking into account the visco-thermal losses at the wall with the hypothesis of large tubes (cf. [7, 11]). The acoustic pressure P and the volume flow U are governed by the following equations, given in the Laplace domain:

$$\left(\frac{s^2}{c^2} + 2\varepsilon(\ell) \frac{s^{\frac{3}{2}}}{c^{\frac{3}{2}}} + \Upsilon(\ell) - \frac{\partial^2}{\partial \ell^2} \right) \{ r(\ell) P(\ell, s) \} = 0, \quad (1)$$

$$\rho s \frac{U(\ell, s)}{S(\ell)} + \frac{\partial}{\partial \ell} P(\ell, s) = 0, \quad (2)$$

where $s \in \mathbb{C}$ is the Laplace variable ($\Im m(s) = \omega$ is the pulsation), ℓ is the curvilinear abscissa at the wall, $r(\ell)$ is the radius of the pipe, $S(\ell) = \pi r(\ell)^2$ is the section area, $\varepsilon(\ell) = \kappa_0 \sqrt{1 - r'(\ell)^2} / r(\ell)$ quantifies the visco-thermal losses ($\text{m}^{-\frac{1}{2}}$) and $\Upsilon(\ell) = r''(\ell) / r(\ell)$ represents the curvature of the pipe. Conical and flared pipes are characterized by $\Upsilon \geq 0$ (e.g. a trumpet horn) and convex pipes by $\Upsilon < 0$. Equation (1) is the *Webster-Lokshin* equation, and (2) is the *Euler* equation satisfied outside the boundary layer.

2.2. Two equivalent systems

We define a piece of pipe by a tube with a finite length L and with constant coefficients of losses and curvature (ε and Υ). We will build two systems which represent the acoustic effects of a piece of pipe on the travelling waves given by:

$$\phi^\pm = \frac{r}{2} (P \pm ZU), \quad \text{where } Z(\ell) = \frac{\rho c}{S(\ell)}. \quad (3)$$

In [4], the effects of a piece of pipe on the variables ϕ^\pm are represented by input/output systems for the *Webster-Lokshin* model. Two equivalent forms (in an input/output point of view) are given.

A first form, so-called ‘‘global’’, is given in Fig. 2-(a). Its 4 transfer functions represent global effects of the piece of pipe on the waves ϕ^\pm : R_g^l and R_g^r are the left and right reflections respectively, and T_g is the global transmission through the piece of pipe. ‘‘global’’ means that all internal acoustic effects are mixed, for example the forwards and backwards components of wave propagation are taken into account.

A second form, so-called ‘‘decomposed’’, is given by Fig. 2-(b). This form is interesting because it isolates the internal acoustic effects inside some transfer functions. For example, R_{le} represents the reflection of ϕ_0^+ at the left interface, and T represents the propagation through the piece of pipe. Here the successive forwards and backwards components are represented by the internal loop. This form allows the recovery of the *Kelly-Lochbaum* framework which is well adapted for digital real-time simulation (cf. e.g. [9]).

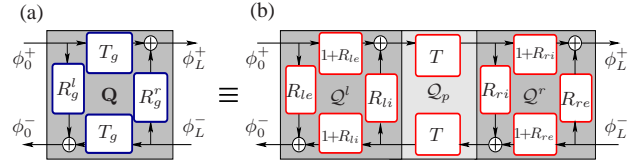


Figure 2: Two-port Q (global form) and its decomposed form.

Let's define $\Gamma(i\omega) = ik(\omega)$, where $k(\omega)$ is the standard complex wavenumber. In the Laplace domain, the function Γ is given by

$$\Gamma(s) = \sqrt{\left(\frac{s}{c}\right)^2 + 2\varepsilon\left(\frac{s}{c}\right)^{\frac{3}{2}} + \Upsilon}. \quad (4)$$

The analytical solving of (1) and (2) gives the functions of Q

$$T_g = \{A_T \cosh(\Gamma L) + B_T \sinh(\Gamma L) / \Gamma\}^{-1}, \quad (5)$$

$$R_g^l = \{A_R \cosh(\Gamma L) + B_{Rl} \sinh(\Gamma L) / \Gamma\} T_g, \quad (6)$$

$$R_g^r = \{A_R \cosh(\Gamma L) + B_{Rr} \sinh(\Gamma L) / \Gamma\} T_g, \quad (7)$$

where A_T , A_R , B_T , B_{Rl} and B_{Rr} are some known functions of s and $\Gamma(s)^2$. With $\zeta = r'/r$, the functions of the decomposed form are given in [4]:

$$T(s) = e^{-\Gamma(s)L}, \quad (8)$$

$$R_{le}(s) = \frac{\frac{s}{c} - \Gamma(s) - \zeta_l}{\frac{s}{c} + \Gamma(s) + \zeta_l}, \quad R_{li}(s) = -\frac{\frac{s}{c} - \Gamma(s) + \zeta_l}{\frac{s}{c} + \Gamma(s) + \zeta_l}, \quad (9)$$

$$R_{re}(s) = \frac{\frac{s}{c} - \Gamma(s) + \zeta_r}{\frac{s}{c} + \Gamma(s) - \zeta_r}, \quad R_{ri}(s) = -\frac{\frac{s}{c} - \Gamma(s) - \zeta_r}{\frac{s}{c} + \Gamma(s) - \zeta_r}. \quad (10)$$

With $\tau := L/c$, note that we can write $T_g(i\omega) = D_g(i\omega) e^{-i\omega\tau}$ and $T(i\omega) = D(i\omega) e^{-i\omega\tau}$, where D_g and D are two transfer functions associated to causal systems (for $\Upsilon \geq 0$). Consequently, the impulse responses of T_g and T are these ones of D_g and D delayed by τ which corresponds to the time of propagation inside the piece of pipe.

In the case of pipes with negative curvatures ($\Upsilon < 0$) these two forms present a paradox: whereas some numerical calculus reveal that the global form of Fig. 2-(a) is stable, the transfer functions of the decomposed form of Fig. 2-(b) have some singularities in the Laplace domain which produces some instabilities. The aim of the following section is a better understanding of the reasons behind this problem.

3. ANALYSIS OF SINGULARITIES

3.1. Complex analysis of Γ

The function $\Gamma(s)$ (associated to the wavenumber $k(\omega)$, cf. (4)) is defined as a square root of a complex number which depends itself on a square root of s . But there is an infinite number of continuations of the positive square root defined on \mathbb{R}^+ for the complex plane, and we must choose one of them in order to define in \mathbb{C} the transfer functions of the system.

In [12, 13], the function Γ is defined by the choice of curves (called *cut*) which link some *branching points* to the infinity. These cuts are continuous sets of singularities, which produce some discontinuities of Γ . And the branching points s_n are the solutions of $\Gamma(s)^2 = 0$, and $s_0 = 0$ (for \sqrt{s}).

$\Upsilon = 0$: For cylindrical and conical pipes, the unique branching point is $s_0 = 0$.

$\Upsilon > 0$: For flared pipes, Γ has 3 branching points: $s_0 = 0$, s_1 and $s_2 = \overline{s_1}$, with $\Re(s_1) \leq 0$.

$\Upsilon < 0$: For convex pipes, Γ has 2 branching points: $s_0 = 0$, and $s_1 \in \mathbb{R}^+$.

Whereas these branching points are fixed (they depend on c , ε and Υ), the cuts have to be chosen.

For $\Upsilon \geq 0$, since no branching point is in the right-half Laplace plane (denoted $\mathbb{C}_0^+ := \{s \in \mathbb{C} / \Re(s) > 0\}$), it is possible to define an analytical continuation over \mathbb{C}_0^+ in order to respect the stability of the transfer functions. For example, the case of horizontal cuts is presented in Fig. 3.

However, for $\Upsilon < 0$, one branching point s_1 is in \mathbb{C}_0^+ , and so it is not possible to define an analytical continuation over \mathbb{C}_0^+ since at least one part of the cut is in \mathbb{C}_0^+ . Figure 3 presents the case of 2 overlapped cuts on $\mathbb{R}^-:]-\infty, 0]$ and $] -\infty, s_1]$.

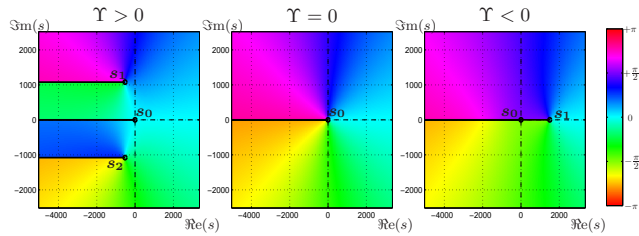


Figure 3: Phase of $\Gamma(s)$ in the complex plane, branching points and horizontal cuts.

3.2. Poles and physical interpretation

Whereas the transfer functions of the decomposed form (cf. (8-10)) have the same type of singularities as Γ (of the cut type), the 3 global transfer functions (cf. (5-7)) only depends on $\Gamma(s)^2$ and not $\Gamma(s)$ (they are invariant with the transformation $\Gamma \mapsto -\Gamma$). Thus these 3 transfer functions have only one cut which comes from \sqrt{s} , and some other singularities of the pole type which are associated to the resonance modes of the piece of pipe.

This last remark implies that only the transfer functions of the decomposed form depend on the choice of Γ . The input/output relations do not depend on the choice of the cuts which start from s_1 and s_2 (because of the curvature) but they only depend on the cut which starts from $s_0 = 0$ (because of the visco-thermal losses). For this branching point, we will choose \mathbb{R}^- for some reasons of stability and hermitian symmetry.

In [14], Γ is given by $\sqrt{\cdot}$ defined by

$$\sqrt{\cdot}: s = \rho \exp(i\theta) \mapsto \sqrt{s} = \sqrt{\rho} \exp(i\theta/2), \quad (11)$$

with $(\rho, \theta) \in \mathbb{R}^{+*} \times]-\pi, \pi]$. With this choice of Γ , the set of the cuts is $\mathbb{R}^- \cup \mathcal{C}$ with $\mathcal{C} := \{s \in \mathbb{C} / \Gamma(s)^2 \in \mathbb{R}^-\}$. With this definition, Γ has the following property:

$$\forall s \in \mathbb{C} \setminus \mathcal{C}, \Re(\Gamma(s)) > 0. \quad (12)$$

Consequently, when L increases,

$$\forall s \in \mathbb{C} \setminus \mathcal{C}, T(s) = e^{-\Gamma(s)L} \rightarrow 0, \text{ when } L \rightarrow \infty. \quad (13)$$

Thus, in the decomposed form of Fig. 2-(b), $T(s)$ behaves as a ‘‘circuit breaker’’ at the limit. And so, we prove the following result

$$\forall s \in \mathbb{C} \setminus \mathcal{C}, \lim_{L \rightarrow \infty} R_g^L(s) = R_{le}(s). \quad (14)$$

The function R_{le} is then interpreted as the global reflection of a semi-infinite pipe (anechoic). A similar reasoning has been done in [3] for cones.

We observe the convergence of poles and zeros of R_g^L towards the cut \mathcal{C} of R_{le} when L increases. Thus, the cut can be interpreted as a densification of intertwined poles and zeros. Figure 4 illustrates this convergence with $\Upsilon > 0$.

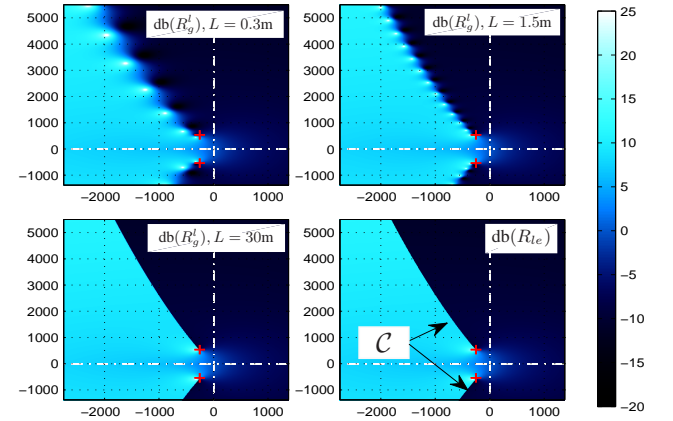


Figure 4: Convergence of poles and zeros of R_g^L when $L \rightarrow \infty$ (with $\Upsilon > 0$). Poles, zeros and branching points are represented by white points, black points and red crosses respectively.

3.3. Interpretation for $\Upsilon < 0$

For negative curvatures, because of the part of the cut on $[0, s_1] \subset \mathbb{R}^+$, the associated functions have an infinite number of singularities which produce instabilities. But some numerical observations show that the global transfer functions of the piece of pipe which do have not this cut, are stable as expected.

A pipe with constant and negative curvature $\Upsilon = r''/r$ has a sinusoidal profile $r(\ell)$ which changes sign every L_{crit} defined by

$$L_{crit} := \pi \sqrt{|\Upsilon|}. \quad (15)$$

But we observe that when L increases, a pole p_k of R_g^L becomes unstable as soon as the length L of the piece of pipe exceeds kL_{crit} (with $k \in \mathbb{N}^*$). Figure 5 illustrates this.

In this case, when $L \rightarrow \infty$ there is a densification of an infinite number of unstable poles on $[0, s_1]$. Thus, for $L < L_{crit}$ the global transfer functions of the piece of pipe are stable, but the transfer functions of the decomposed form, which are associated to a semi-infinite pipe, have an infinite number of unstable singularities. This phenomenon comes from the decomposition of Fig. 2-(b) which is well adapted to digital waveguide simulations with positive curvatures. For negative curvatures we have to search for another decomposition which is adapted to waveguides and which is stable for $\Upsilon < 0$.

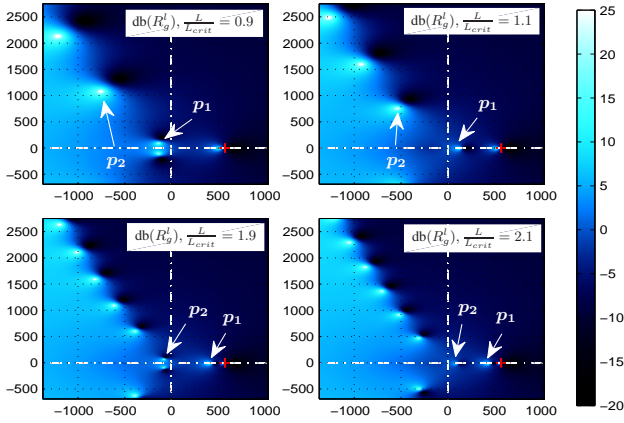


Figure 5: Pole transition from \mathbb{C}_0^- to \mathbb{R}^+ , with $\Upsilon < 0$.

4. GENERALIZED FRAMEWORK

In this section, we show that the 2 forms (global and decomposed) can be represented by a common framework which is parameterized by 2 degrees of freedom which are 2 transfer functions of the system. Then in the next section, we propose 2 parameters which guarantee the stability.

4.1. Global form and decomposed form

We have seen that the piece of pipe can be modelled by 2 systems (cf. Fig. 2). The first is given by the two-port \mathbf{Q} and its 4 global functions; and the second is given by a decomposed form with 10 transfer functions.

- **Global form:** No matter the sign of the curvature coefficient Υ , the transfer functions R_g^l , R_g^r , and T_g are stable. Moreover, we have seen that they have only one cut on \mathbb{R}^- because of the visco-thermal losses. Their simulation with a modal approach, could allow a stable realization of the piece of pipe. But low-cost computation requires the truncation of modes, which involves some problems of realism.
- **Decomposed form:** This form is adapted to waveguide modelling, but it implies some problems of stability. With $\Upsilon < 0$ an unstable part of the cut appears on \mathbb{R}^+ .

In the next section, we see that there is an infinite number of forms of a piece of pipe, and then we get a parametrization in order to find a stable realization which respects the waveguide formalism.

4.2. Standard form of a piece of pipe

First, we represent the 2 forms of Fig. 2 with a common framework: the framework of Fig. 6 is equivalent to the 2 forms (global or decomposed) if the following equations hold:

- Global form:

$$\begin{aligned} \mathcal{H}_l &= R_g^l, & \mathcal{F}_l &= D_g, & \mathcal{G}_l &= 0, \\ \mathcal{H}_r &= R_g^r, & \mathcal{F}_r &= D_g, & \mathcal{G}_r &= 0. \end{aligned}$$
- Decomposed form:

$$\begin{aligned} \mathcal{H}_l &= R_{le}, & \mathcal{F}_l &= D(1 + R_{ri})(1 + R_{le}), \\ \mathcal{H}_r &= R_{re}, & \mathcal{F}_r &= D(1 + R_{li})(1 + R_{re}), \\ \mathcal{G}_l &= \frac{R_{li}D(1 + R_{ri})}{1 + R_{li}}, & \mathcal{G}_r &= \frac{R_{ri}D(1 + R_{li})}{1 + R_{ri}}. \end{aligned}$$

where D and D_g correspond to the transmissions T and T_g without delay: $T(s) = D(s)e^{-\tau s}$ and $T_g(s) = D_g(s)e^{-\tau s}$. The other functions of the decomposed form are given by (8-10).

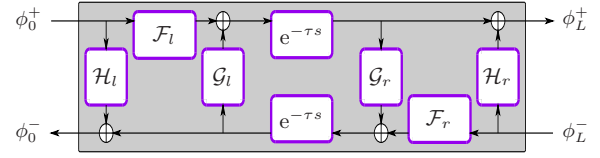


Figure 6: Standard form of a piece of pipe

4.3. Parametrization

In a general case, the standard form (Fig. 6) allows the representation of a piece of pipe if the following algebraic equations hold

$$R_g^l = \mathcal{H}_l + \frac{\mathcal{F}_l \mathcal{G}_r e^{-2\tau s}}{1 - \mathcal{G}_l \mathcal{G}_r e^{-2\tau s}}, \quad (16)$$

$$R_g^r = \mathcal{H}_r + \frac{\mathcal{F}_r \mathcal{G}_l e^{-2\tau s}}{1 - \mathcal{G}_l \mathcal{G}_r e^{-2\tau s}}, \quad (17)$$

$$D_g = \frac{\mathcal{F}_l}{1 - \mathcal{G}_l \mathcal{G}_r e^{-2\tau s}}, \quad (18)$$

$$= \frac{\mathcal{F}_r}{1 - \mathcal{G}_l \mathcal{G}_r e^{-2\tau s}}. \quad (19)$$

We observe that this system of equations has 2 degrees of freedom. Choosing \mathcal{G}_l and \mathcal{G}_r as degrees of freedom, the solving of the system (16-19) gives

$$\mathcal{H}_l = R_g^l - D_g \mathcal{G}_r e^{-2\tau s}, \quad (20)$$

$$\mathcal{H}_r = R_g^r - D_g \mathcal{G}_l e^{-2\tau s}, \quad (21)$$

$$\mathcal{F}_l = D_g (1 - \mathcal{G}_l \mathcal{G}_r e^{-2\tau s}), \quad (22)$$

$$\mathcal{F}_r = D_g (1 - \mathcal{G}_r \mathcal{G}_r e^{-2\tau s}). \quad (23)$$

Consequently, it is possible to choose arbitrarily the functions \mathcal{G}_l and \mathcal{G}_r and to preserve the original input/output relations of the system. And so we have a parametrization of the system with 2 functions. For example the global form corresponds to the choice: $\mathcal{G}_l = 0, \mathcal{G}_r = 0$.

In the case of the decomposed form, the 6 transfer functions have no internal delay, the modes of the piece of pipe are simulated by the loop. For the global form, $\mathcal{G}_l = \mathcal{G}_r = 0$, the loop is open, and the modes are simulated by the delays in the denominator of the 4 other functions.

Remarks: For all causal and stable \mathcal{G}_l and \mathcal{G}_r , the 4 functions \mathcal{H}_l , \mathcal{H}_r , \mathcal{F}_l and \mathcal{F}_r defined by (16-19) are causal and stable. Moreover, the choice \mathcal{G}_l and \mathcal{G}_r such as $|\mathcal{G}_l(s)| < 1$ and $|\mathcal{G}_r(s)| < 1, \forall s \in \mathbb{C}_0^+$, allows the guarantee of the stability of the internal loop of the system.

Now we have to find \mathcal{G}_l and \mathcal{G}_r which allow to guarantee the stability and the passivity of the system, and to preserve the waveguide formalism.

5. STABLE REALIZATION OF CONVEX PIPE

5.1. Stabilization of convex pipes

With the waveguide approach, the “ideal” choice is this one of the decomposed form. With

$$R_{li}^* := \frac{R_{li}(1 + R_{ri})}{1 + R_{li}} D \quad \text{and} \quad R_{ri}^* := \frac{R_{ri}(1 + R_{li})}{1 + R_{ri}} D, \quad (24)$$

this “ideal” choice is given by $\mathcal{G}_l = R_{li}^*$ and $\mathcal{G}_r = R_{ri}^*$. But these functions depend on Γ and they have some unstable singularities on $[0, s_1]$ with $\Upsilon < 0$. We should make another choice.

5.1.1. What can be a “good choice”?

Qualitatively, in order to understand what is a “good choice” of \mathcal{G}_l and \mathcal{G}_r we can examine for example the expression of the function \mathcal{F}_l given by (22):

$$\mathcal{F}_l(s) = D_g(s) (1 - \mathcal{G}_l(s)\mathcal{G}_r(s) e^{-2\tau s}).$$

The function D_g has a cut on \mathbb{R}^- because of losses, and an infinite number of pairs of complex conjugate poles in \mathbb{C}_0^- . Every pair corresponds to a mode of the piece of pipe. These poles are the zeros of the denominator of D_g which is: $1 - R_{li}^* R_{ri}^* e^{-2\tau s}$. The choice $\mathcal{G}_l = R_{li}^*$ and $\mathcal{G}_r = R_{ri}^*$, allows the exact compensation of the poles of D_g . With this choice, \mathcal{F}_l has no pole as singularity, but only the cut \mathcal{C} of Γ .

The idea we propose and test here, is to compensate the high frequency poles (there is a infinite number) by the internal loop of the framework with a choice such as $\mathcal{G}_l(i\omega) \approx R_{li}^*(i\omega)$ and $\mathcal{G}_r(i\omega) \approx R_{ri}^*(i\omega)$ when $|\omega|$ is high, but with \mathcal{G}_l and \mathcal{G}_r holomorphic in \mathbb{C}_0^+ . Finally, the staying poles which are not compensated in low frequencies are simulated as such in the 4 transfer functions $\mathcal{H}_l, \mathcal{H}_r, \mathcal{F}_l$ and \mathcal{F}_r given by (20-23).

5.1.2. How to find a “good choice”?

For simplification, we artificially modify the functions R_{li}^* and R_{ri}^* with a mapping $s \mapsto \gamma(s)$ of the complex plane:

$$\mathcal{G}_l(s) := R_{li}^*(\gamma(s)), \quad \text{and} \quad \mathcal{G}_r(s) := R_{ri}^*(\gamma(s)). \quad (25)$$

Now the choice of \mathcal{G}_l and \mathcal{G}_r is done by the choice of this “mapping”. To guarantee a good behavior in high frequency ($\mathcal{G}_l(i\omega) \approx R_{li}^*(i\omega)$ and $\mathcal{G}_r(i\omega) \approx R_{ri}^*(i\omega)$), we choose γ such as:

$$\forall s \in \overline{\mathbb{C}_0^+} \text{ with } |s| \text{ high: } \gamma(s) \approx s. \quad (26)$$

Remark: The expression “ $|s|$ high” is voluntarily imprecise. In practice, we want that $\gamma(i\omega)$ goes *quickly* towards $i\omega$ when $|\omega|$ increases.

5.1.3. Properties of a “good mapping”

Not only does γ have to verify (26), but it is also interesting to control the singularities of \mathcal{G}_l and \mathcal{G}_r with the choice of γ . First, the chosen mapping has to guarantee the stability and the passivity of \mathcal{G}_l and \mathcal{G}_r , and if possible it has to reduce the set of their singularities. To guarantee the good definition of these functions, we give some constraints:

P1: γ is hermitian (for real signals),

P2: γ is analytical in \mathbb{C}_0^+ ,

P3: $]-\infty, s_1] \cap \gamma(\mathbb{C}_0^+) = \{\emptyset\}$,

P4: $\forall s \in \mathbb{C}_0^+, |R_{li}^*(\gamma(s))| < 1$ and $|R_{ri}^*(\gamma(s))| < 1$.

With these properties, the choice $\mathcal{G}_l(s) := R_{li}^*(\gamma(s))$ and $\mathcal{G}_r(s) := R_{ri}^*(\gamma(s))$ defines some hermitian functions (P1), holomorphic in \mathbb{C}_0^+ (P2, P3 and because R_{li}^* and R_{ri}^* are holomorphic on $\mathbb{C} \setminus]-\infty, s_1]$) and P4 guarantees the stability of the loop.

Note that the set of the cuts of \mathcal{G}_l and \mathcal{G}_r becomes $\mathcal{C}^\dagger := \{s \in \mathbb{C} / \gamma(s) \in]-\infty, s_1]\}$ (with $\mathcal{C}^\dagger \subset \mathbb{C}_0^-$ thanks to P3). Thus the mapping γ allows the “rejection” of the unstable part of the cut of Γ ($[0, s_1] \subset \mathbb{R}^+$) in \mathbb{C}_0^- , and this stabilizes the transfer functions.

5.2. Stable digital realization

Now we give some results of stable realizations of a piece of pipe with a negative curvature. We use the previous idea, but with some empirical considerations.

The procedure is summarized by the following steps:

- We choose the parameter functions \mathcal{G}_l and \mathcal{G}_r using a mapping γ .
- We deduce $\mathcal{H}_l, \mathcal{H}_r, \mathcal{F}_l$ and \mathcal{F}_r .
- We approximate the 6 transfer functions using standard recursive filters.

5.2.1. Definition of the mapping

In practice, instead of looking for a well defined γ in \mathbb{C} , we limit the search in $i\mathbb{R}$ (Fourier domain). Thus, we look for a contour given by $\gamma(i\mathbb{R})$.

In high frequencies, the contour must get closer to the imaginary axis (cf. (26)), and so we choose it such as $\gamma(i\omega) = i\omega$ with $|\omega| > \omega_0$, where ω_0 is a pulsation we can name *junction pulsation*.

In lower frequencies, this contour has not only to get around the part $[0, s_1]$ of the cut (to guarantee P3), but also to get around the set of $s \in \mathbb{C}$ such as $|R_{li}^*(s)| > 1$ and $|R_{ri}^*(s)| > 1$ (P4).

Moreover, this contour must verify a constraint of \mathcal{C}^∞ -regularity on $i\mathbb{R}$ (necessary condition for P2). Thus, the “junction” at $\omega = \pm\omega_0$ between low and high frequencies must have the continuity of all its derivatives.

In order to simulate only the 2 first modes of the piece of pipe, the junction pulsation ω_0 is chosen equal to $\Im m(p_2)$ where p_2 is the pole associated to the second mode of the piece of pipe.

Figure 7 illustrates the contour $\gamma(i\omega)$ which gets around the cut, and the contour line of 1.

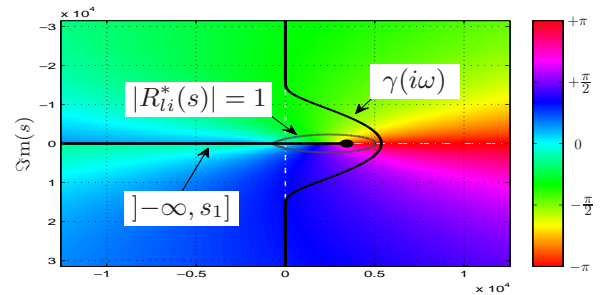


Figure 7: Phase of R_{li}^* and contour $\gamma(i\omega)$.

5.2.2. Approximation and results

Previously, we have chosen a mapping γ which defines the parameter functions \mathcal{G}_l and \mathcal{G}_r . Then, we deduce \mathcal{H}_l , \mathcal{H}_r , \mathcal{F}_l and \mathcal{F}_r which preserve the input/output relations of the system using (20-23). For a given piece of pipe this choice allows the definition of a system composed by stable transfer functions, and which contains a stabilized delay loop ($|\mathcal{G}_l| < 1$ and $|\mathcal{G}_r| < 1$ in \mathbb{C}_0^+), cf. Fig. 6.

For the digital realization of the system, first the transfer functions \mathcal{G}_l and \mathcal{G}_r are approximated by standard recursive filters. This type of approximation is presented in [12, 13, 16]; here it needs a placement of some poles on \mathbb{R}^- .

For \mathcal{H}_l , \mathcal{H}_r , \mathcal{F}_l and \mathcal{F}_r , the same type of approximation is realized. Here, with $|\omega| > \omega_0$, $\mathcal{G}_l(i\omega) = R_{li}^*(i\omega)$ and $\mathcal{G}_r(i\omega) = R_{ri}^*(i\omega)$, in consequence the modes with frequencies higher than ω_0 are simulated by the internal loop of the system. Then, there are two staying modes (in low frequencies) which are simulated by 2 pairs of complex conjugate poles.

For evaluation, we have built the realization of a convex piece of pipe with the following parameters: $r_0 = 7$ cm, $r_L = 10$ cm, $\Upsilon = -100$ m⁻², $L = 15$ cm, and $\varepsilon = 0.0033$ m^{-1/2}. The junction pulsation is fitted according to the second mode of the piece of pipe which corresponds to a pair of poles at $\omega_0 \approx 17 \cdot 10^3$ rad.s⁻¹ ($F_0 = \omega_0/(2\pi) \approx 2700$ Hz). Every transfer function \mathcal{G}_l or \mathcal{G}_r is simulated by 6 stable poles (on \mathbb{R}^-) and every function among the 4 other by 6 stable real poles and 2 pairs of complex conjugate poles. The delays of the framework of Fig. 6 are simulated by low-cost digital delays (circular buffers) of 19 samples ($F_s L/c \approx 19$ with $F_s = 44100$ Hz is the sample rate).

Figure 9 illustrates the frequency response of \mathcal{H}_l and its approximation. We observe 2 lobes which correspond to the 2 first resonances of the piece of pipe which are not simulated by the internal loop.

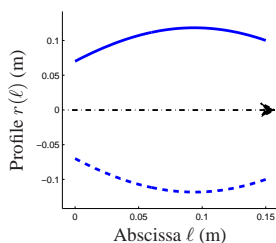


Figure 8: Profile of the simulated convex pipe.

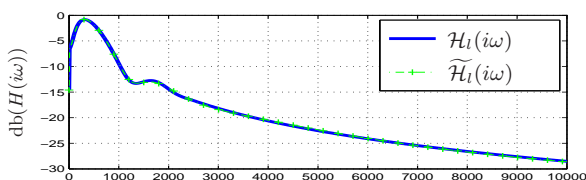


Figure 9: \mathcal{H}_l and its approximation $\widetilde{\mathcal{H}}_l$.

The result of the simulation is illustrated in Fig. 10 by the frequency response of the global transfer function R_g^r and of its simulated version \widetilde{R}_g^r . Note that the maximal error is almost 1.9 dB, and its mean is 0.3 dB.

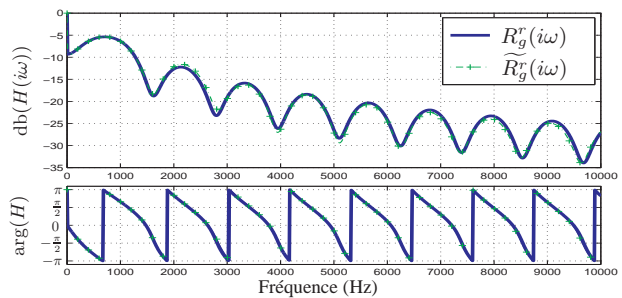


Figure 10: R_g^r and its simulated version \widetilde{R}_g^r .

6. CONCLUSION

In this paper, we have seen in the case of convex pipes that the use of the simulation framework of [4] produces some problems of stability, because of the presence of unstable singularities which are not of the pole type, but of the *cut* type. After an explanation of the problem, we have proposed a “generalized” framework which parameterizes the system with 2 degrees of freedom which are 2 transfer functions. Then in part 5 we have done a choice which stabilizes the system and preserves the approach of [4]. This choice allows the “rejection” of the unstable singularities to the left-half Laplace plane, and this stabilizes them. Finally, the digital simulation of a piece of pipe has been realized with 2 delays and 6 standard recursive filters.

The stable simulation is obtained thanks to two key points: first, the piece of pipe is represented with the new decomposition proposed in Fig. 6; second, the two degrees of freedom of this decomposition (here, chosen as \mathcal{G}_l and \mathcal{G}_r) are tuned through a parameterized contour $\omega \mapsto \gamma(i\omega)$ so that the internal reflection functions do not contain singularities in \mathbb{C}_0^+ and have their modulus smaller than 1 in \mathbb{C}_0^+ . In future work, the choice of the mapping γ could be improved to guarantee additional properties such that γ maps all the singularities to \mathbb{R}^- only.

Moreover, only the stability of one piece of pipe is done. For the simulation of a whole virtual pipe, which is the concatenation of several pieces of pipe, it is necessary to study the stability of the whole system. This could be achieved proving the passivity of the digital system for a piece of pipe, and proving that this passivity property is preserved after the connection with another passive system.

7. REFERENCES

- [1] D. P. Berners, *Acoustics and signal processing techniques for physical modeling of brass instruments*. PhD thesis, Stanford University, 1999.
- [2] V. Pagneux, *Propagation acoustique dans les guides à section variable et effet d'écoulement*. PhD thesis, Université du Maine, 1996.
- [3] J. Gilbert, J. Kergomard, and J.-D. Polack, “On the reflection functions associated with discontinuities in conical bores,” *J. Acoust. Soc. Am.*, vol. 87, no. 4, pp. 1773–1780, 1990.
- [4] T. Hélie, R. Mignot, and D. Matignon, “Waveguide modeling of lossy flared acoustic pipes: Derivation of a Kelly-Lochbaum structure for real-time simulations,” in *IEEE WASPAA*, (Mohonk, USA), pp. 267–270, 2007.

- [5] J. O. Smith, "Music applications of digital waveguides," Tech. Rep. STAN-M-39, Center for Computer Research in Music and Acoustics (CCRMA), Department of Music, Stanford University, 1987.
- [6] A. Webster, "Acoustic impedance and the theory of horns and of the phonograph," *Proc. Nat. Acad. Sci. U.S.*, vol. 5, pp. 275–282, 1919.
- [7] J.-D. Polack, "Time domain solution of Kirchhoff's equation for sound propagation in viscothermal gases: a diffusion process," *J. Acoustique*, vol. 4, pp. 47–67, February 1991.
- [8] T. Hélie, "Unidimensional models of acoustic propagation in axisymmetric waveguides," *J. Acoust. Soc. Am.*, vol. 114, pp. 2633–2647, 2003.
- [9] J. D. Markel and A. H. Gray, "On autocorrelation equations as applied to speech analysis," *IEEE Trans. Audio and Electroac.*, vol. 21, April 1973.
- [10] http://fr.wikipedia.org/wiki/Fichier:HA_Lorée.jpg.
- [11] A. A. Lokshin and V. E. Rok, "Fundamental solutions of the wave equation with retarded time," *Dokl. Akad. Nauk SSSR*, vol. 239, 1978.
- [12] G. Montseny, "Diffusive representation of pseudo-differential time-operators," *ESAIM: Proc.*, vol. 5, pp. 159–175, 1998.
- [13] T. Hélie, D. Matignon, and R. Mignot, "Criterion design for optimizing low-cost approximations of infinite-dimensional systems: Towards efficient real-time simulation," in *IFAC Workshop on Control Applications of Optimisation (CAO'06)*, (Cachan, France), 2006. 6 pages.
- [14] R. Mignot, T. Hélie, and D. Matignon, "On the appearance of branch cuts for fractional systems as a mathematical limiting process based on physical grounds," in *IFAC Fractional Differentiation and its Applications*, (Ankara, Turkey), 2008. 6 pages.
- [15] V. Pagneux, N. Amir, and J. Kergomard, "A study of wave propagation in varying crosssection waveguides by modal decomposition. Part I: Theory and validation," *J. Acoust. Soc. Am.*, vol. 100, no. 4, pp. 2034–2048, 1996.
- [16] R. Mignot, T. Hélie, and D. Matignon, "Digital waveguide modeling for wind instruments: building a state-space representation based on the webster-lokshin model," *IEEE Transactions on Audio, Speech and Language Processing*, vol. 18, pp. 843–854, May 2010.